The low ionic strength crystal structure of horse cytochrome *c* at 2.1 Å resolution and comparison with its high ionic strength counterpart

R Sanishvili[1], KW Volz[2], EM Westbrook[3] and E Margoliash[1]*

[1]Laboratory for Molecular Biology, Department of Biological Sciences, The University of Illinois at Chicago, 845 W. Taylor St., Chicago, IL 60607, USA, [2]Department of Microbiology and Immunology, The University of Illinois at Chicago, 835 S. Wolcott Ave., Chicago, IL 60612, USA and [3]Biological and Medical Research Division, Argonne National Laboratory, 9700 S. Cass Ave., Argonne, IL 60439, USA

Background: Cytochrome *c* is an integral part of the mitochondrial respiratory chain. It is confined to the intermembrane space of mitochondria, and has the function of transferring electrons between its redox partners. Solution studies of cytochrome *c* indicate that the conformation of the molecule is sensitive to the ionic strength of the medium.

Results: The crystal structures of cytochromes *c* from several species have been solved at extremely high ionic strengths of near-saturated solutions of ammonium sulfate. Here we present the first crystal structure of ferricytochrome *c* at low ionic strength refined at 2.1 Å resolution. In general, the structure has the same features as those determined earlier. However, there are some differences in both backbone and side-chain conformations in several areas. These areas coincide with those observed by NMR and resonance Raman spectroscopy to be sensitive to ionic strength.

Conclusions: Neither ionic strength nor crystal-packing interactions have much influence on the conformation of horse cytochrome *c*. Nevertheless, some differences in the side-chain conformations at high and low ionic strengths may be important for understanding how the protein functions. Close examination of the γ-turn (residues 27–29) conserved in cytochromes *c* leads us to propose the 'negative classical' γ-turn to describe this unusual feature.

Structure 15 July 1995, **3**:707–716

Key words: cytochrome *c*, γ-turn, high ionic strength structure, internal water molecules, low ionic strength structure

Introduction

Cytochrome *c* is a small, heme-containing protein encoded by the nuclear genome that carries out its physiological function in the intermembrane space of mitochondria. It is the substrate for a number of physiological reductants (cytochrome *c* reductase, cytochrome b_5, sulfite oxidase and cytochrome b_2) and oxidants (cytochrome *c* oxidase and cytochrome *c* peroxidase) [1–3], thus playing a crucial role in a variety of mitochondrial redox systems. The three-dimensional structure of cytochrome *c* was one of the first protein structures to be solved by X-ray diffraction methods [4]. The structures of the protein from several species are now available, including baker's yeast, rice, tuna, bonito and horse [5–12].

Cytochrome *c* has been used extensively not only in studies of the respiratory chain of mitochondria and related electron transport systems, but also as a model for the study of experimental approaches and phenomena that are applicable to all proteins. In the vast majority of these investigations horse cytochrome *c* was employed, and its atomic structure has been essential to the interpretation of much of this work. The structure of horse cytochrome *c* was originally solved by Dickerson and coworkers [4] and then further refined to higher resolution by Bushnell *et al.* [11]. Here, the first structure of cytochrome *c* solved at close to physiological ionic strength is reported. It is important to obtain the structure under these conditions because all earlier determinations were carried out with crystals obtained in near-saturated ammonium sulfate. There are observations indicating that the conformation of some areas of cytochrome *c* is dependent on the ionic strength of the medium. For example, Feng and Englander's [13] NMR spectroscopic analysis demonstrated that residues 61, 83 and 87–89 are influenced by the salt concentration. Interestingly, many of these residues are located in, or close to, the enzymatic interaction domain, namely the surface area involved in the interactions with the multiple redox partners of cytochrome *c*, as determined by chemical modification studies [14] and X-ray crystallography [15]. Using ultraviolet resonance Raman spectroscopy, Liu *et al.* [16] detected that Tyr48 and Trp59 were affected by changing the ionic strength. These two residues are important components of the heme crevice and thus critical for forming the native environment for the buried heme. Pelletier and Kraut [15] observed that the side-chain conformation of Gln16 in the complex with cytochrome *c* peroxidase (CcP) differs from that in the free protein at high ionic strength. They attributed this difference to the different ionic strengths used in crystallization, rather than to complex formation. Small-angle X-ray scattering studies [17] showed that the radius of gyration of cytochrome *c* varies at different ionic strengths, indicating an expansion of the molecule at lower ionic strengths. On the other hand, an X-ray study of lysozyme T4 [18] demonstrated that there was no conformational dependence of this protein on ionic

*Corresponding author.

strength. Thus, the present work examines whether the conformation of the cytochrome *c* molecule is sensitive to the ionic strength of the medium, and if so, what are the changes that occur. Furthermore, studies of horse cytochrome *c* in complex with Fab fragments of specific monoclonal antibodies, crystallized at low ionic strength are now in progress [19]. Accurate comparisons of free and complexed cytochrome *c* molecules require its structure to be determined from crystals grown under similar, low ionic strength, conditions.

Results

Overall structure

The crystal structure of horse ferricytochrome *c* was solved in space group $P2_12_12_1$ at an ionic strength of ~65 mM. It was refined to 2.1 Å resolution to an R-factor of 17.7% (Table 1) and a root mean square (rms) deviation from ideal bond lengths and angles of 0.017 Å and 0.057° respectively. There are two protein molecules in the asymmetric unit, denoted A and B. The (ϕ,ψ) angles of all residues fall within the permitted regions of the Ramachandran plot (data not shown), except for several glycines and Lys27 (discussed below). In Figure 1 the distribution of temperature factors, averaged separately over residue backbones and side-chain atoms, is shown. As discussed below, molecule B is somewhat disordered and does not refine as well as molecule A. Therefore further analysis of the structure is based on molecule A, unless molecule B is specifically referred to.

The structure of horse cytochrome *c* at low ionic strength maintains all the major features characteristic of the cytochromes *c* from different species previously solved at high ionic strength as follows. The heme is sandwiched between the right side (residues 1–48, 93–104) and the left side (residues 49–92) of the protein (Fig. 2), and is attached by two covalent thioether bonds to the sulfur atoms of Cys14 and Cys17. The protoporphyrin ring of the heme is buried in a hydrophobic crevice and its propionyl side chains form an extensive network of hydrogen bonds with the rest of the protein (Table 2). His18 and Met80 provide the axial ligands of the heme iron. The protein contains three long α-helices and two short ones, six type II β-turns, one unusual γ-turn and two short segments of 3_{10}-helix (Table 3).

The side chains of four residues (Lys7, Lys53, Lys72 and Lys73) in molecule A and five residues (Lys7, Lys39, Lys53, Lys72 and Lys100) in molecule B have rotamers

Table 1. Distribution of R-factors and of the number of reflections greater than 2σ over the resolution shells.

Resolution limits (Å)	No. of reflections predicted	No. of unique reflections, I>2σ	R_f (%)
10.0–4.70	1082	1000	18.6
4.70–3.70	1207	1116	12.8
3.70–3.20	1261	1161	15.2
3.20–2.90	1219	1048	17.7
2.90–2.65	1467	1088	20.6
2.65–2.35	2672	1177	22.9
2.35–2.08	3893	1094	26.6
10.0–2.08	12801	7684	17.7

The incompleteness of the data at high resolution is caused by the short life-time of the crystals in the X-ray beam and settings of the area detector preventing the measurement of the weaker reflections in the higher resolution shells.

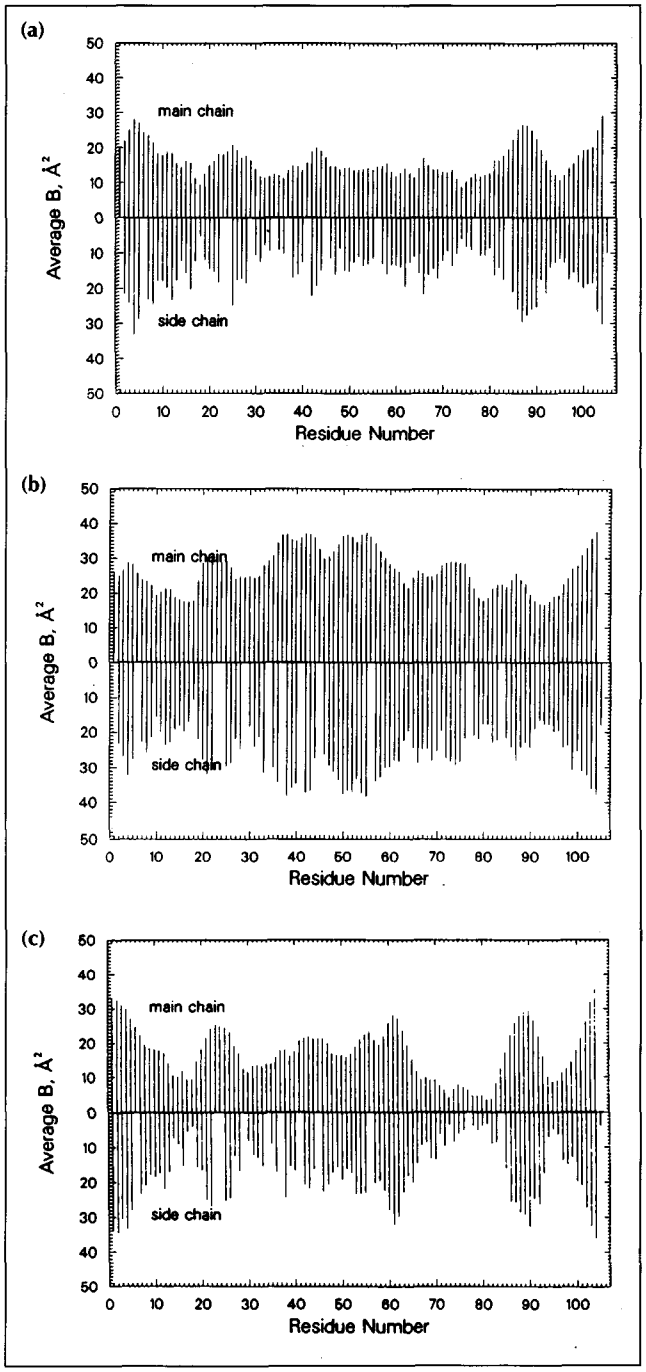

Fig. 1. Plot of the temperature factors *versus* the residue number of horse cytochrome *c* for **(a)** molecule A, **(b)** molecule B and **(c)** the molecule at high ionic strength. The temperature factors are averaged for main-chain and side-chain atoms separately. The heme is presented as a side chain (residue number 105).

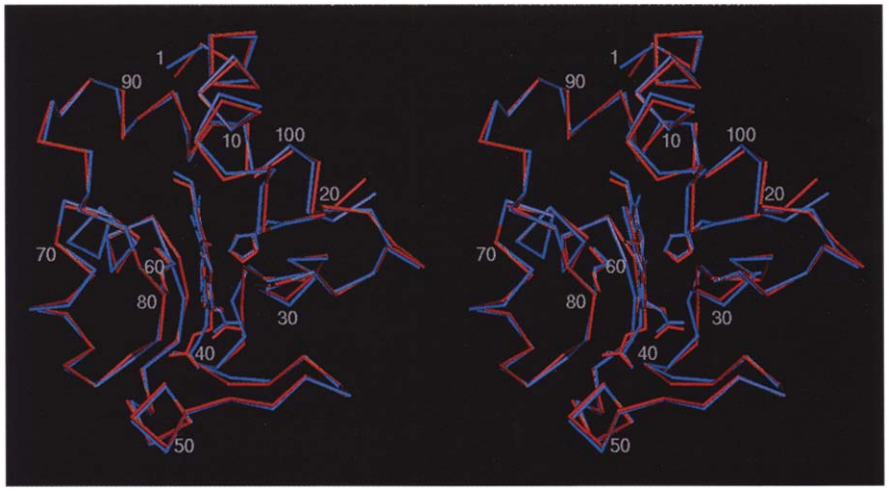

Fig. 2. Superposition of Cα skeletons of horse ferricytochrome *c* at high (blue) and low (red) ionic strengths. The N and C termini and every tenth Cα atom are labeled. The heme, together with the side chains of its two axial ligands, His18 and Met80, are also shown.

Table 2. Possible hydrogen bonds between the heme and the rest of the horse cytochrome *c* molecule at low ionic strength.

Heme atom	Protein atom		D–A distance (Å)	D–H–A angle (°)
O2A	NH	Gly41	2.7	164
O2A	Nδ2	Asn52	2.8	134
O1A	OH	Tyr48	2.9	–
O1A	OH	Wat107	2.7	–
O2D	NH	Lys79	2.6	144
O2D	Oγ1	Thr78	2.4	–
O2D	Oγ1	Thr49	2.7	–
O1D	Oγ1	Thr49	2.8	–
O1D	NH	Thr49	2.9	176

In the automatic search, the length of hydrogen bonds was limited to 3.25 Å and the maximum deviation from linearity of the D–H–A angle was limited to 60°, where D, A and H denote donor, acceptor and proton, respectively. The hydrogen-bond angles are not given for the hydroxyl groups of water, tyrosine and threonine, because the correct locations of their protons are not known.

with clearly distinct conformations. The side chains of three more residues (Glu61, Lys86 and Lys100) in molecule A, and five more (Lys5, Lys22, Glu61, Lys88, Glu92) in molecule B, could also be fitted to the electron density in more than one conformation, of similar orientation, probably indicating mobility or structural disorder of these side chains.

The solvent molecules

In the later stages of refinement, 133 water molecules were included in the model. Out of these, 75 are associated with molecule A and another 58 with molecule B. Three water molecules, Wat106, Wat107 and Wat108, are buried in the cytochrome *c* structure forming an extensive hydrogen-bond network with the protein (Table 4). The stability of these water molecules is reflected in their temperature factors, which are the lowest of all the water molecules associated with molecule A. These three waters are also present in the structure of horse cytochrome *c* obtained at high ionic strength [11]. One of them, Wat106, is thought to be important for the function of the protein [7,12,20,21]. The role of Wat107 is poorly understood other than its 'architectural' significance [7] in consolidating the bottom portion on the right side of the protein (as viewed in Fig. 2). Nevertheless, one could assume that it is important for protein function as it forms a hydrogen bond with the anterior propionic acid of the heme. One of its possible roles might be to maintain the conformation of the side chain of Arg38, which is directed towards the molecule interior. It is thought to be involved in setting the reduction potential of the protein by charge–charge interactions with the heme posterior propionate and/or by hydrogen bonding to it mediated by Wat107 [3,22,23]. The third buried molecule, Wat108, stabilizes the conformation of the γ-turn formed by residues 27–29. It may also have functional significance as the conformational stability of the γ-turn and the adjacent residues appears to be important for the stability of the protein and of the coordination of the heme iron by the sulfur of Met80 [24,25]. Several water molecules occupying more than one position were also detected. The corresponding electron densities are dumbbell shaped and larger than would be expected for a single molecule.

Interactions of the α-helices

The intramolecular hydrogen bonds and hydrophobic interactions involving the atoms of the five α-helices are listed in Table 5. A remarkable feature of the horse cytochrome *c* structure, as well as of those solved earlier, is a continuous network of interactions involving these α-helices as they encircle the heme. Thus, α_1 is connected to α_5, α_5 to α_3, and α_3 to α_4 and α_2. Helix α_1, even though it is the second longest in horse cytochrome *c*, forms a somewhat poor network of interactions, compared with the other helices, leading to relatively high temperature factors of this segment of the polypeptide chain (Fig. 1). An important function of this helix seems to be stabilization of α_5 and Phe10 is undoubtedly the major contributor, acting as a hydrophobic anchor among a number of non-polar side chains from helix α_5 (Table 5). Helix α_1 also covers the heme from the top-right side and is covalently bound to it via Cys14. Helix α_5 covers the hydrophobic back edge of the heme and interacts with α_1

Table 3. Elements of secondary structure in horse cytochrome *c* at low and high ionic strengths.

Secondary structure	Low ionic strength		High ionic strength*	
	Residue range	$(\phi,\psi)^{\dagger}$	Residue range	$(\phi,\psi)^{\dagger}$
α_1	2–14	–74,–34	6–14	–76,–36
3_{10}	14–17	–25,–46; –57,–33	14–17	–44,–29; –56,–38
$\beta_{II}^{\ddagger}$	21–24	–76,116; 108,–20	21–24	–67,125; 96,7
γ	27–29	–55,–48		–100,–47#
β_{II}	32–35	–69,143; 73,15	32–35	–64,147; 49,7
β_{II}	35–38	–53,106; 112,–4	35–38	–51,130; 67,7
$\beta_{II}^{\ddagger\S}$	39–42	–72,161; 53,35		–63,139; 62,47#
$\beta_{II}^{\ddagger}$	43–46	–69,143; 72,4		–73,150; 71,0#
α_2	49–55	–63,–37	49–54	–61,–47
α_3	60–69	–63,–41	60–69	–55,–50
3_{10}	67–70	–58,–23; –67,–32	67–70	–39,–49; –62,–27
α_4	70–75	–70,–31	70–75	–55,–55
β_{II}	75–78	–91,141; 76,27	75–78	–62,112; 111,–14
α_5	87–104	–68,–43	87–102	–61,–43

The residue ranges and (ϕ,ψ) values at high ionic strength were taken from Table 3 in [11]. †The values of (ϕ,ψ) dihedral angles are given as follows: for the α-helices, the average value for all the residues is given; for the β-turns and 3_{10}-helices those of the i+1 and i+2 residues are given, and for the γ-turn, that of residue i+1 is given. ‡These are open β-turns where the conformations of the residues fulfill the β_{II}-turn definition but the required hydrogen bond is absent [30]. §In this turn the required hydrogen bond is achieved by water molecule 107, bridging the carbonyl oxygen of Lys39 and the amide nitrogen of Gln42. #These elements are not listed in [11] but they have essentially the same conformation as in our crystals.

Table 4. Hydrogen bonds formed by the water molecules buried in the protein globule.

Water molecule	Temperature factor (Å^2)	Hydrogen bonds to		Length of hydrogen bond (Å)
106	6.0	Oδ1	Asn52	2.3
		OH	Tyr67	2.7
		Oγ1	Thr78	2.8
107	11.7	Nε	Arg38	2.4
		Nη1	Arg38	3.1
		O	Lys39	3.0
		N	Gln42	3.0
		O1A	Heme	2.7
108	13.4	O	Lys25	2.6
		N	Lys27	3.1
		O	Gly29	2.8

as well as several other areas of the molecule, including helix α_3. Helix α_3 plays a very significant structural role, covering the heme from the left-rear side and placing Tyr67 in the heme crevice. Helix α_4, on the left-front side of the heme, forms a great number of hydrophobic interactions, mainly via Tyr74 and Ile75. Finally, helix α_2 is the only one of five helices which approaches the heme from beneath, where the two propionyl side chains are directed. As a consequence, this helix displays almost no hydrophobic contacts with the rest of the protein but instead forms a large number of hydrogen bonds. These include several bonds with the heme itself and with the internal water molecule, Wat106 (Tables 2,5).

Remarkably, neither His18 nor Met80, which provide the axial ligands of the heme iron, reside on any of the five α-helices. Nevertheless, they have quite stable conformations, as judged from their temperature factors (Fig. 1). The major contributors to the stability of His18 appear to be two hydrogen bonds, one between the amide nitrogen of His18 and the carbonyl oxygen of Cys14 and the other between Nδ1 of His18 and the carbonyl oxygen of Pro30; and, of course, coordination of its Nε2 atom to the heme iron. It is also surrounded by residues Phe10, Cys14, Ala15, Val20, Leu32 and the heme, preventing the movement of the imidazole side chain. Met80 is stabilized mainly by van der Waals contacts with the heme, coordination of its Sδ atom with the heme iron and the hydrogen bond formed between the hydroxyl of Tyr67 and Sδ of Met80. However, Met80 is partially exposed to the solvent and it can occupy a potential cavity inside the protein by displacing Wat106 [21]. Consequently, Met80 has a greater degree of freedom than His18 and is a weaker ligand of the heme iron, as was demonstrated by ligation of the heme with various exogenous ligands and by heat and pH titrations of ferricytochrome *c* (see [3] and references therein).

The cytochromes *c* from different species have relatively short polypeptide chains, being little more than 100 residues long. At the same time, the heme has to be well covered to exclude the external solvent, thus requiring some sharp turns of the polypeptide chain. The large number of turns (9) and glycines (12) in horse cytochrome *c* probably serve to relieve the resulting conformational tension required to achieve compact wrapping of the heme.

Discussion

The greater disorder of molecule B

There are several indications that molecule B is disordered in the crystal. First, in the Lattman rotation function the

Table 5. Intramolecular interactions involving the five α-helices in horse cytochrome *c* at low ionic strength.

Helix	Hydrogen-bonding atoms				Distance (Å)	Hydrophobic interactions between residue pairs		
α_1	N	Asp2	Oδ1	Asp93	2.9	Val3–Ala96	Ile9–Leu94	Phe10–Leu98
	Oδ2	Asp2	N	Val3	3.2	Lys7–Tyr97	Phe10–Leu94	Phe10–Val20
						Ile9–Glu90	Phe10–Tyr97	
α_2	N	Thr49	O1D	Heme	2.9	Lys55–Ile57		
	Oγ1	Thr49	O	Thr49	3.0	Lys55–Ile75		
	Oγ1	Thr49	O1D	Heme	2.8			
	Oγ1	Thr49	O2D	Heme	2.7			
	Oδ1	Asp50	Nζ	Lys53	2.6			
	Oδ1	Asn52	O	Wat106	2.3			
	Nδ2	Asn52	O2A	Heme	2.8			
	Nζ	Lys55	O	Tyr74	2.6			
α_3	Oε1	Glu61	Nζ	Lys99	3.0	Lys60–Trp59	Leu64–Ile95	Tyr67–Leu68
	Oγ1	Thr63	O	Thr58	2.6	Thr63–Ile57	Met65–Ile95	Tyr67–Pro71
	Oγ1	Thr63	N	Lys60	2.6	Leu64–Phe36	Glu66–Tyr74	Leu68–Leu94
	OH	Tyr67	O	Wat106	2.7	Leu64–Trp59	Tyr67–Trp59	
	O	Leu68	N	Ile85	2.7			
α_4	Nζ	Lys72	O	Ala83	3.2	Pro71–Tyr67	Tyr74–Glu66	Ile75–Lys55
	Nζ	Lys72	O	Met80	2.8	Pro71–Met80	Tyr74–Tyr67	Ile75–Pro76
	Nζ	Lys72	O	Phe82	2.6	Tyr74–Ile57	Tyr74–Ile75	Ile75–Thr78
	O	Tyr74	N	Lys55	2.6	Tyr74–Thr63	Ile75–Ala51	
α_5	Nε	Arg91	O	Ile85	3.0	Arg91–Leu68	Ile95–Leu64	Tyr97–Phe10
	Nη2	Arg91	O	Lys86	2.4	Asp93–Ile9	Ile95–Met65	Leu98–Phe10
	Nη1	Arg91	O	Met65	3.3	Leu94–Ile9	Ala96–Gly1	Leu98–Phe36
	Oδ1	Asp93	N	Asp2	2.9	Leu94–Gly6	Ala96–Val3	Ala101–Val20
	OH	Tyr97	O	Wat109	3.2	Leu94–Ile85	Tyr97–Lys7	Thr102–Leu32
	Nζ	Lys99	Oε2	Glu61	3.2	Leu94–Phe10		
	O	Thr102	N	Gly34	3.0			

The hydrogen bonds forming the helices are not listed.

peak corresponding to this molecule was smeared, stretching from α=23° to α=30°. Second, although the variation of the temperature factors over the polypeptide chain is similar in both molecules A and B (compare Figs 1a,b), the temperature factor values are considerably larger in molecule B, indicating a higher degree of disorder. Differences in the intermolecular contacts may explain this effect. The two molecules in contact are involved in a similar number of such interactions. In the case of molecule A, the majority of these contacts are produced by backbone atoms. Only two such main-chain contacts are observed for molecule B. Clearly, this allows molecule B to be more mobile than molecule A.

The γ-turn in cytochromes *c*

The tight turn, formed by residues 27–29, exists in all cytochromes *c* whose structures have been solved (Table 6). It is not mentioned in some publications (see, for example, [7,8,11,26]), or is identified as a classical γ-turn [10]. Ochi and co-workers [9] list this element as a "compact reverse turn". It has the same conformation as a classical γ-turn except that the first peptide is 'flipped over' (Fig. 3). It also has several features, associated with classical γ-turns. Thus, all the side chains are on one side of the plane that passes through the Cα atoms of the turn [27]. Although residue 29 is a glycine in our case, the β-hydrogen atom is on the same side as the side chains of Lys27 and Thr28. Another feature of classical γ-turns is a reversal of chain direction [27,28]. In horse cytochrome *c*, the distance between the Cα atoms of the residues immediately before and after this turn is 4.4 Å, indicating such a chain reversal. Nevertheless, the turn in cytochrome *c* is not a classical γ-turn as no hydrogen bond exists between the carbonyl of the first residue (Lys27) and the amide nitrogen of the last (Gly29). Instead, a hydrogen bond is formed between the backbone amide nitrogen of Lys27 and the carbonyl oxygen of Gly29 (Fig. 3b). A turn containing such a bond, and described as resembling a γ-turn [28], is found in bovine pancreatic trypsinogen [29]. In our case, the turn does not resemble a classical γ-turn because both dihedral angles at the middle (i+1) residue, are negative (Table 6), and one of the criteria for such γ-turns is that $\phi_{i+1}>0°$ and $\psi_{i+1}<0°$ [27,28,30]. It could be suggested that the criteria for the γ-turn definition be revised, in which case the turn in cytochromes *c* could be called, for example, a 'negative classical' γ-turn, emphasizing the fact that both dihedral angles at the middle residue have negative values.

It should be noted that such turns are likely to be a rarity in proteins. Indeed, one of the reasons for, or results of, such an unusual γ-turn is that the backbone

Table 6. The backbone conformational angles (°) of γ-turns in cytochromes *c* from different species.

Source	Entry code in PDB	Sequence of the γ-turn	ϕ_i,ψ_i	ϕ_{i+1},ψ_{i+1}	ϕ_{i+2},ψ_{i+2}
Horse ferric low ionic strength	1CRC	KTG	−121, −136	−55, −48	−99, 155
Horse ferric high ionic strength	1HRC	KTG	−76, -92	−100, −47	−91, 162
Tuna ferric	3CYT	KVG			
Inner molecule			−112, −129	−65, −37	−113, 167
Outer molecule			−105, −132	−56, −40	−115, 170
Tuna ferros form*	5CYT	KVG	−71, −60	−134, −49	−97, 175
Yeast iso-1ferric	2YCC	KVG	−129, −123	67, −56	−97, 168
Yeast iso-1 ferros	2YCC	KVG	−123, −128	−57, −49	−103, 165
Yeast iso-2 ferros	1YEA	KVG	−158, −138	59, −46	−106, 170
Rice ferric	1CCR	KQG†	−132, −143	−59, −41	−108, 164

*The (ϕ,ψ) angle values for this protein may not be reliable because the corresponding ω angles differ considerably from 180°. Thus, ω_i=171°, ω_{i+1}=163° and ω_{i+2}=177°. †Sequence numbers of residues forming the γ-turn are 35–37.

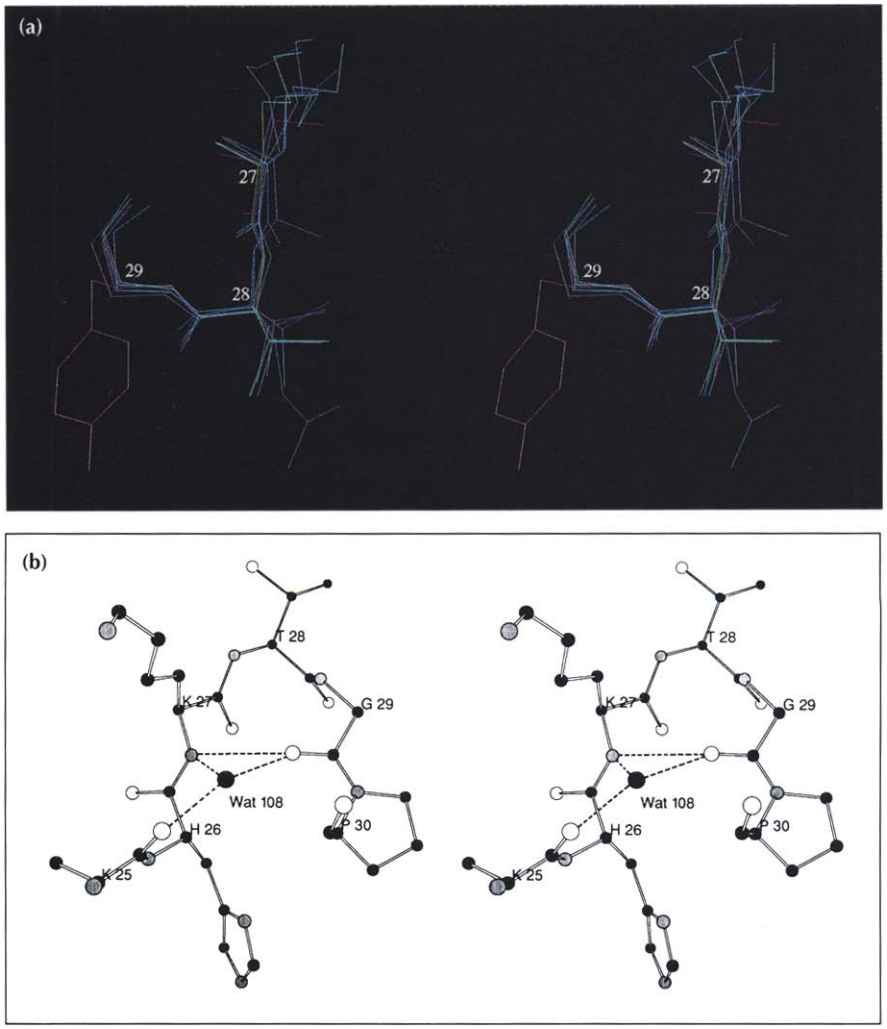

Fig. 3. The γ-turn. **(a)** Stereo superposition of the γ-turns formed by residues 27–29 in cytochromes *c* and cytochrome c_2 from *Rhodospirillum rubrum* [41] with the classical γ-turn from thermolysin. Different shades of blue correspond to the turns in the oxidized form of tuna, rice, yeast, horse (high ionic strength) and *R. rubrum* proteins. Green corresponds to the turn in horse cytochrome *c* at low ionic strength and the classical γ-turn is shown in magenta. **(b)** Stereo diagram of the γ-turn in cytochromes *c*. Atoms are coded as follows: carbons, black; oxygens, white and nitrogens, gray. The larger black sphere represents the water molecule Wat108. The residues are labeled at their Cα atoms. The dashed lines show the hydrogen bonds stabilizing the conformation of the turn.

conformation of its first residue, Lys27, is energetically unfavorable and falls outside the permitted regions on a Ramachandran plot. It is partially compensated for by the hydrogen bonds formed by Nζ of Lys27 to the carbonyl oxygen of residue 15 and possibly also to residue 16. This interaction also exists in yeast cytochrome *c* [10], although it is not discussed in the report of the high ionic strength structure of the horse protein [11]. In addition to the hydrogen bonds stabilizing Lys27, the γ-turn in cytochrome *c* is involved in several hydrogen bonds. These are the bonds within the turn, mediated by the water molecule, Wat108 (Fig. 3b), and the hydrogen bond between the amide nitrogen of Gly29 and the carbonyl of Cys17. Another water molecule, Wat110, mediates the hydrogen bonds between the amide nitrogen of Thr28, the carbonyl of Gln16 and the hydroxyl of Thr28.

Comparison of the structures of horse cytochrome *c* at low and high ionic strengths

This study of ionic strength effects on the structure of horse cytochrome *c* is based on the present work and coordinates kindly provided to us by G Brayer [11]. It is clear from Figure 2 and Table 4 that the overall fold of the molecule does not change even when the ionic strength of the crystallization medium varies from ~65 mM to ~15 M. Indeed, the rms displacement of all Cα atoms after least-squares superpositioning was 0.476 Å, which is even less than that for two molecules in the asymmetric unit of the low ionic strength crystals (0.490 Å). Interestingly, the pattern of temperature factor variation along the polypeptide chain remains quite close in these two structures (compare Figs 1a,c). This is a further demonstration that the intrinsic structural features of a protein molecule are not significantly changed by differences in crystal lattice packing. Large differences are not expected as numerous intramolecular interactions, stabilizing a protein structure, are overwhelmingly stronger than a few intermolecular contacts in a crystal. These stabilizing interactions are also strong enough to eliminate the major influence of ionic strength, at least above 50 mM.

Nevertheless, there are some differences in both backbone and side-chain conformations. Many of them cannot be discounted from a functional point of view even if they seem insignificant from purely structural considerations. For instance, both the N- and C-terminal α-helices are longer in the low ionic strength structure as they include additional residues at both ends. The conformation of these areas is similar at both ionic strengths but in the high ionic strength structure the terminal turns of the helices are stretched (Fig. 2), breaking the hydrogen bonds required to qualify them as α-helical.

Pelletier and Kraut [15] observed that the conformation of the Gln16 side chain of horse cytochrome *c* differs in the complex with CcP, whose structure was solved at very low ionic strength (5 mM), from that in the free protein at high ionic strength. This side chain folds back and forms a hydrogen bond with its own backbone amide nitrogen in the complex, whereas in the free protein at high ionic strength it extends towards the heme. The authors assigned this difference to the different ionic strengths in the crystallization medium rather than to complex formation. From the present structure it appears that the side chain of Gln16 of free cytochrome *c* can have both conformations. Indeed, in molecule A it has the same conformation as in the complex with CcP, and in molecule B the conformation is similar to that of free cytochrome *c* at high ionic strength (Fig. 4). This side chain is likely to be mobile under physiological conditions and it is possible that a high salt concentration forces it into one conformation, while complex formation with CcP forces it into the other. The mobility of Gln16 could have an important physiological role as it controls solvent accessibility of the exposed edge of the heme. The surface area accessible to solvent is less for the methyl group of the upper anterior pyrrole ring (3.3 $Å^2$) and β-carbon of the same pyrrole (18.7 $Å^2$) in molecule B than in molecule A. The corresponding values in molecule A are 7.3 $Å^2$ and 28.0 $Å^2$. Furthermore, Gln16 is located near the center of the enzymatic interaction domain of cytochrome *c* and is invariant in all species with known amino acid sequences [3], except for the highly divergent cytochrome *c* of *Tetrahymena pyriformis*.

The change in side-chain conformation of Gln16 also appears to be correlated with movements of the side chains of Ile81 and Phe82 (Fig. 4). Thus, the back-folded conformation of the Gln16 side chain (molecule A) is associated with the smallest angle between the planes of the Phe82 phenyl ring and the heme and the closest approach of Ile81 to the solvent-exposed heme edge. By contrast, the extended side chain of Gln16 (high ionic strength structure) occurs with the largest angle between the heme and phenyl planes and the furthest displacement of Ile81 from the heme edge. The intermediate conformation of the Gln16 side chain (seen for molecule B) is correlated with similarly intermediate conformations of Phe82 and Ile81. The possible involvement of Gln16 in modifying the conformations of Ile81 and Ph82 and in the physiological activity of the protein could be tested by site-directed mutagenesis.

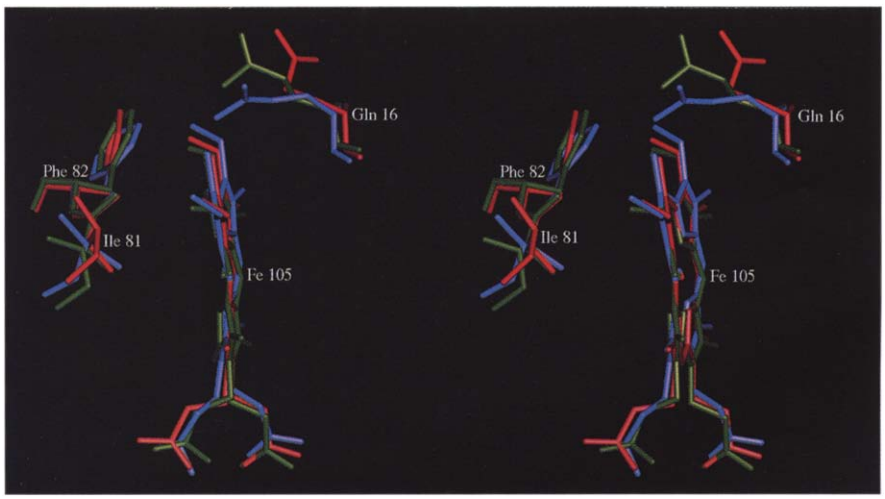

Fig. 4. Different conformations of the Gln16 side chain at low ionic strength in molecule A (red), molecule B (green) and at high ionic strength (blue). The orientation is close to the 'standard' view, as shown in Figure 2.

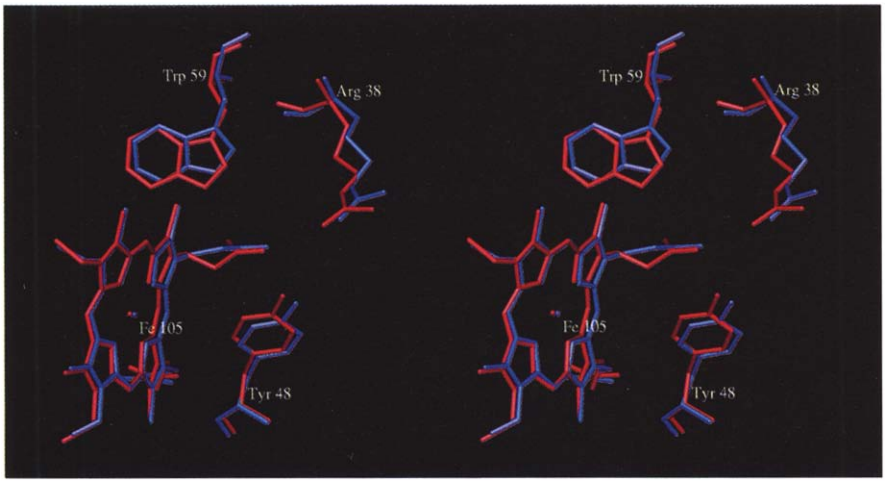

Fig. 5. Comparison of the conformations of Arg38, Tyr48 and Trp59 at low (red) and high (blue) ionic strength. At low ionic strength all three side chains are further from the posterior heme propionic acid. The view is from the top-right side of the molecule.

There are interesting differences between the conformations of Arg38, Tyr48 and Trp59 in horse cytochrome *c* at low and high ionic strengths (Fig. 5). These groups, approaching the heme from three different directions, are further from it at low ionic strength, obviously indicating some expansion of the lower right part of the molecule. Such a sensitivity of Arg38, Tyr48 and Trp59 to the ionic strength seems to be very important as these residues are part of the immediate heme environment and are considered to be significant for the physicochemical properties of the molecule [3,22,23]. Liu *et al.* [16] demonstrated by ultraviolet resonance Raman spectroscopy that the hydrogen/deuterium exchange rate for the Nϵ1 of the indole side chain of Trp59 in horse cytochrome *c* decreases dramatically upon increase of ionic strength. Indeed, the hydrogen bond between this Nϵ1 and the heme propionic acid side chain is absent in the low ionic strength structure of horse cytochrome *c*. Even if this bond exists, it will be extremely weak because of its length (3.3 Å). In contrast, at high ionic strength the bond length is practically ideal (2.7 Å). The absence of this interaction, or its weakness, explains the observed increase in the hydrogen/deuterium exchange rate with the decrease of ionic strength, because a proton involved in forming a hydrogen bond is less available for exchange. Liu *et al.* also suggest that at very low ionic strength (5 mM), the hydrogen bond between the hydroxyl of Tyr48 and the posterior propionyl side chain of the heme is absent. The length of this bond is 2.4 Å and 3.0 Å at high and low ionic strengths, respectively. It is possible that as the ionic strength decreases from ~15 M to ~65 mM in the two crystal structures, this bond becomes weaker, and finally, at very low ionic strength it is broken, as observed by Liu *et al.* [16].

Feng and Englander [13] identified residues Glu61, Ala83, Lys87, Lys88 and Thr89 as displaying the largest salt-dependent changes. The comparison of the X-ray structures of high and low salt crystals revealed no significant conformational differences in this region, even though there are some differences in the interactions of the neighboring residues. Thus, at low ionic strength Arg91 forms hydrogen bonds with carbonyl oxygens of Lys85, Lys86 and Met65 (Fig. 6). Furthermore, its guanidinium group is stacked with the carboxylate group of Glu69, interacting with it electrostatically, the distances from the Nη1 and Nη2 of Arg91 to the Oϵ2 and Oϵ1 atoms of Glu69 being 3.8 Å and 4.4 Å respectively. With these interactions, Arg91 clearly contributes to stabilization of the protein, forming a bridge between two α-helices, α_3 and α_5. Some of these interactions appear to be absent at high ionic strength and could represent examples of the influence of ionic strength on electrostatic interactions at the protein surface.

Biological implications

Cytochrome *c* is an integral part of the mitochondrial respiratory system and is therefore crucial for living organisms. It has been studied by a wide variety of methods, over several decades, both with a view to understanding the mechanism of electron transport and as a model protein system.

The structures of several cytochromes *c* from different species have been solved and refined at high resolution from crystals grown at the extremely high ionic strengths of near-saturated solutions of ammonium sulfate. The current atomic model, obtained at close to physiological salt concentrations, can serve as a structural basis for interpreting the results of a number of experiments, as well as for theoretical investigations and predictions of different features of the protein.

Several earlier studies demonstrated that cytochrome *c* displays structural sensitivity to the ionic strength of the medium. The dependence of the structure of lysozyme on the ionic strength of the medium has been addressed crystallographically [18] and no significant conformational differences were observed. Here the same question is addressed in the case of cytochrome *c* which, because of its highly charged surface, is potentially more sensitive to ionic strength, making it attractive for such studies.

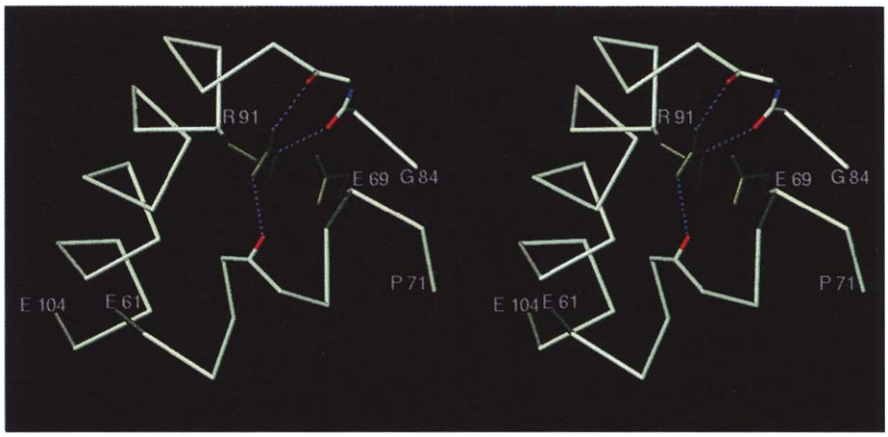

Fig. 6. Stabilizing interactions involving Arg91. Two helices, α_3 and α_5, are represented by their Cα atoms. Also shown are the carbonyls (red) of Met65, Ile85 and Lys86 and the side chains (green) of Glu69 and Arg91. Possible hydrogen bonds formed by the guanidinium group of Arg91 are shown as blue dashed lines.

We find that the overall structure of cytochrome *c* does not change even when the ionic strength varies between ~65 mM and ~15 M. However, care should be taken when a protein structure is analyzed from the functional point of view, as some parts of a molecule can be responsive to the salt concentration of the medium. We present several examples of such responses, which may influence our understanding of functional mechanisms and stabilization of molecular structure. For example, the different interactions at high and low ionic strengths of the residues Arg38, Tyr48 and Trp59 with the heme prosthetic group may change our estimation of their contribution to the stability of the immediate environment of the heme and of the protein molecule as a whole. Knowledge of these interactions under physiological conditions may help us to define the electronic structure of the heme more accurately, and hence the coordination of axial ligands and possibly also the mechanism of electron transfer. The mobility of the Gln16 side chain, regulating solvent exposure of the heme, could have a role in modulating electron transfer.

In addition, we analyzed the properties of a γ-turn, present in all cytochromes *c* of known three-dimensional structure, leading us to propose a broadening of the definition of classical γ-turns.

Materials and methods

Crystallization and data collection

Crystallization of horse heart cytochrome *c* at low ionic strength and data collection have been described previously [31]. Briefly, crystals were obtained by a macroseeding procedure from solutions of polyethylene glycol (PEG). We used the vapor diffusion technique [32] in both sitting and hanging drop applications. The drops contained ~30 mg ml^{-1} protein and 20–25% (w/v) PEG1000 in 0.05 M potassium phosphate buffer, pH 7.0. The wells contained the same buffer with ~30% PEG. The crystals grew in the space group $P2_12_12_1$ with lattice parameters a=55.62 Å, b=105.01 Å and c=35.11 Å and two molecules per asymmetric unit. These parameters were measured on a CAD4 diffractometer (Enraf Nonius). Crystallographic diffraction data were collected on a Siemens/Xentronics multiwire area detector [33] and reduced with the program package XENGEN [34]. Crystals of other cytochromes *c* have been obtained in this space group only twice, but with lattice parameters different from those presented here. They were a=57.68 Å, b=84.58 Å and c=37.83 Å for bonito cytochrome *c* [5], and a=63.1 Å, b=91.4 Å and c=36.7 Å for the tuna protein [6]. The three-dimensional structure was solved only for the crystals of bonito cytochrome *c*.

Structure solution

The structure of horse ferricytochrome *c* was solved by molecular replacement with the program package MERLOT [35] running on μVAX II computer. The coordinates of tuna ferricytochrome *c* [8] from the Protein Data Bank [36] were used as an initial model with the following modifications. First, 14 of the 18 residues which differ between the horse and tuna proteins were changed to alanines. Of the remaining four residues, Gly89 was left unchanged and Val28, Tyr46 and Val58 were modified into the corresponding residues of the horse protein, Thr28, Phe46 and Thr58. Also four lysine residues with high temperature factors were truncated to alanines. The remaining atoms constitute ~90% of horse cytochrome *c*.

Calculation of the Crowther rotation function of MERLOT for reflections with intensities greater than 3σ in the 8.0–4.0 Å resolution shell resulted in the two strongest peaks at 100% and 95.6% (on an arbitrary scale) with 86.1% for the next strongest peak, and the highest noise peak at 60%. The two strongest peaks provided an internally consistent solution, corresponding to the two molecules in the asymmetric unit, referred to as molecule A and molecule B. These solutions were then refined by the Lattman rotation function using 1° increments for all three angles. The translation function was calculated for the models, pre-oriented according to two sets of rotational angles. It gave one peak for each orientation as expected, but the resulting R-factor in the 8–4 Å resolution shell was an unacceptably high 60%. The R-factor was checked for different pairs of molecules in which all possible 1/2 translations (eight in total) were added to the translation function solution, corresponding to one of the molecules (molecule B). The unambiguous solution yielding an R-factor of 41.1% was obtained for the pair in which the translation vector for the second molecule was $t_{2x}+1/2$, $t_{2y}+1/2$, t_{2z}, where t_{2x}, t_{2y}, t_{2z} are the components of the original translation vector for this molecule. The R-factors for the other seven pairs ranged from 57.1% to 63.3%. After two runs of R-factor minimization for the correct solution, the R-factor was lowered to 36.2%.

Refinement

The model was refined with the program package PROLSQ/PROFFT [37,38] first on a μVAX II and later on an Indigo^2 Extreme workstation. Most of the missing side chains were restored during the first two model inspections using $2F_o-F_c$ and F_o-F_c maps, and the remainder were added later. The final R-factor for the 7684 reflections greater than 2σ in the 10–2.1 Å resolution shell is 17.7% (Table 1). The number of reflections/number of variables ratio for the structure was 1.03 counting only one position for all residues and 0.98 counting rotamers. All model building and subsequent analysis was carried out using the programs FRODO [39] on an Evans & Sutherland PS300, and O [40] on an Indigo^2 Extreme.

Atomic coordinates have been deposited in the Brookhaven Protein Data Bank. The entry identification code is 1CRC.

Acknowledgements: We thank G Brayer (Department of Biochemistry, University of British Columbia) for sending us the coordinates of horse cytochrome *c* at high ionic strength; B Finzel, (Upjohn Co., Michigan) for generously providing us with a UNIX version of the program PROFFT; P Fitzgerald (Merck Research Laboratories, New Jersey) for useful discussions on the results of molecular replacement and M Johnson (Department of Medical Chemistry and Pharmacology, the University of Illinois at Chicago) for providing the computer graphics facility used in the early stages of refinement. This work was supported by NIH grants GM 19121 and AI 12001 to EM.

References

1. Margoliash, E. & Schejter, A. (1966). Cytochrome *c*. *Adv. Protein. Chem.* **21**, 113–286.
2. Pettigrew, G.W. & Moore, G.R. (1987). *Cytochromes c: Biological Aspects.* Springer-Verlag, Berlin and Heidelberg, Germany.
3. Moore G.R. & Pettigrew G.W. (1990). *Cytochromes c: Evolutionary, Structural and Physiological Aspects.* Springer-Verlag, Berlin and Heidelberg, Germany.
4. Dickerson, R.E., *et al.*, & Margoliash, E. (1971). Ferricytochrome *c*. I. General features of the horse and bonito proteins at 2.8 Å resolution. *J. Biol. Chem.* **246**, 1511–1535.
5. Tanaka, N., Yamane, T., Tsukihara T., Ashida, T. & Kakudo, M. (1975). The crystal structure of bonito (katsuo) ferrocytochrome *c* at 2.3 Å resolution. *J. Biochem. (Tokyo)* **77**, 147–162.
6. Swanson, R., Trus, B.L., Mandel. G., Kallai, O.B. & Dickerson, R.E. (1977). Tuna cytochrome *c* at 2.0 Å resolution. I. Ferricytochrome structure analysis. *J. Biol. Chem.* **252**, 759–775.
7. Takano, T. & Dickerson R.E. (1981). Conformation change of cytochrome *c*. I. Ferrocytochrome structure refined at 1.5 Å resolution. *J. Mol. Biol.* **153**, 79–94.
8. Takano, T. & Dickerson R.E. (1981). Conformation change of cytochrome *c*. II. Ferricytochrome *c* structure refinement at 1.8 Å and comparison with the ferrocytochrome structure. *J. Mol. Biol.* **153**, 95–115.
9. Ochi, H., Hata, Y., Tanaka, N. & Kakudo, M. (1983). Structure of rice ferricytochrome *c* at 2.0 Å resolution. *J. Mol. Biol.* **166**, 407–418.
10. Louie, G.V. & Brayer G.D. (1990). High resolution refinement of yeast iso-1-cytochrome *c* and comparisons with other eukaryotic cytochromes *c*. *J. Mol. Biol.* **214**, 527–555.
11. Bushnell, G.W., Louie G.V. & Brayer, G.D. (1990). High-resolution three-dimensional structure of horse heart cytochrome *c*. *J. Mol. Biol.* **214**, 585–595.
12. Berghuis, A.M. & Brayer, G.D. (1991). Oxidation state-dependent conformational changes in cytochrome *c*. *J. Mol. Biol.* **223**, 959–976.
13. Feng, Y. & Englander, W. (1990). Salt-dependent structure change and ion binding in cytochrome *c* studied by two-dimensional proton NMR. *Biochemistry* **29**, 3505–3509.
14. Margoliash, E. & Bosshard, H. (1983). Guided by electrostatics a textbook protein comes of age. *Trends Biochem. Sci.* **93**, 316–320.
15. Pelletier, H. & Kraut, J. (1992). Crystal structure of a complex between electron transfer partners, cytochrome *c* peroxidase and cytochrome *c*. *Science* **258**, 1748–1755.
16. Liu, G., Grygon, C.A. & Spiro, T.E. (1989). Ionic strength dependence of cytochrome *c* structure and Trp-59 H/D exchange from ultraviolet resonance raman spectroscopy. *Biochemistry* **28**, 5046–5050.
17. Trewhella, J., Carlson, V.A.P., Curtis, E.H. & Heidorn, D. (1988). Differences in the solution structures of oxidized and reduced cytochrome *c* measured by small-angle X-ray scattering. *Biochemistry* **27**, 1121–1125.
18. Bell, J.A., Wilson, K.P., Zhang, X.-J., Feber, H.R., Nicholson, H. & Matthews, B.W. (1991). Comparison of the crystal structure of bacteriophage T4 lysozyme at low, medium, and high ionic strengths. *Proteins* **10**, 10–21.
19. Jemmerson, R., Sanishvili, R., Buron, S., Westbrook, E., Westbrook M. & Margoliash, E. (1994). Crystallization of two monoclonal Fab fragments of similar amino-acid sequence bound to the same area of horse cytochrome *c* and interacting by potentially distinct mechanisms. *Acta Crystallogr. D* **50**, 64–70.
20. Luntz, T.L., Schejter, A., Garber, E.A.E. & Margoliash, E. (1989). Structural significance of an internal water molecule studied by site-directed mutagenesis of tyrosine-67 in rat cytochrome *c*. *Proc. Natl. Acad. Sci. USA* **86**, 3524–3528.
21. Schejter, A., Koshy, T.I., Luntz, T.L., Sanishvili, R., Vig, I., & Margoliash, E. (1994). Effects of mutating Asn-52 to isoleucine on the heme-linked properties of cytochrome *c*. *Biochem. J.* **302**, 95–101.
22. Cutler, R.L., *et al.*, & Mauk, A.G. (1989). Role of arginine-38 in regulation of the cytochrome *c* oxidation–reduction equilibrium. *Biochemistry* **28**, 3188–3197.
23. Davies, A.M., *et al.*, & Moore, G.R. (1993). Redesign of the interior hydrophilic region of mitochondrial cytochrome *c* by site-directed mutagenesis. *Biochemistry* **32**, 5431–5435.
24. Koshy, T.I., Luntz, T.L., Schejter, A. & Margoliash, E. (1990). Changing the invariant proline-30 of rat and *Drosophila melanogaster* cytochromes *c* to alanine or valine destabilizes the heme crevice more than the overall conformation. *Proc. Natl. Acad. Sci. USA* **87**, 8697–8701.
25. Qin, W., Sanishvili, R., Plotkin, B., Schejter, A. & Margoliash, E. (1995). The role of histidines 26 and 33 in the structural stabilization of cytochrome *c*. *Biochim. Biophys. Acta*, in press.
26. Mandel N., Mandel, G., Trus, B.L., Rosenberg, G.C., & Dickerson, R.E. (1977). Tuna cytochrome *c* at 2.0 Å resolution. III. Coordinate optimization and comparison of structures. *J. Biol. Chem.* **252**, 4619–4636.
27. Nemethy, G. & Printz, M.P. (1972). The γ-turn, a possible folded conformation of the polypeptide chain. Comparison with the β-turn. *Macromolecules* **5**, 755–758.
28. Milner-White, E.J., Ross, B.M., Ismail, R., Belhadj-Mostefa, K. & Poet, R. (1988). One type of gamma-turn, rather than the other gives rise to chain reversal in proteins. *J. Mol. Biol.* **204**, 777–782.
29. Kossiakoff, A.A., Chambers, J.L., Kay, L.M., & Stroud, R.M. (1977). Structure of bovine trypsinogen at 1.9 angstroms resolution. *Biochemistry* **16**, 654–664.
30. Rose, G.D., Gierash, L.M. & Smith, J.A. (1985). Turns in peptides and proteins. *Adv. Protein Chem.* **37**, 1–109.
31. Sanishvili, R.G., Margoliash, E., Westbrook, M.L., Westbrook, E.M., & Volz, K.W. (1994). Crystallization of wild type and mutant ferricytochromes *c* at low ionic strength: seeding technique and X-ray diffraction analysis. *Acta Crystallogr. D* **50**, 687–694.
32. McPherson, A. (1989). *Preparation and Analysis of Protein Crystals.* Krieger Publishing Co., Malabar, FL.
33. Durbin, R.M., *et al.*, & Wiley, D.C. (1986). Protein, DNA, and virus crystallography with a focused imaging proportional counter. *Science* **232**, 1127–1132.
34. Howard, A.J., Gilliland, G.L., Finzel, B.C., Poulos, T.L., Ohlendorf, D.H. & Salemme, F.R. (1987). The use of an imaging proportional counter in macromolecular crystallography. *J. Appl. Crystallogr.* **20**, 383–387.
35. Fitzgerald, P.M.D. (1988). MERLOT, an integrated package of computer programs for the determination of crystal structures by molecular replacement. *J. Appl. Crystallogr.* **21**, 273–278.
36. Bernstein, F.C., *et al.*, & Tasmui, M. (1977). The protein databank: a computer-based archival file for macromolecular structures. *J. Mol. Biol.* **112**, 535–542.
37. Hendrickson, W.A. (1985). Stereochemically restrained refinement of macromolecular structures. *Meth. Enzymol.* **115**, 252–270.
38. Finzel, B.C. (1987). Incorporation of fast Fourier transforms to speed restrained least-squares refinement of protein structures. *J. Appl. Crystallogr.* **20**, 53–55.
39. Jones, T.A. (1978). A graphics model building and refinement system for macromolecules. *J. Appl. Crystallogr.* **11**, 268–272.
40. Jones, T.A., Zou, J.Y., Cowan, S.W. & Kjeldgaard, M. (1991). Improved methods for building protein models in electron density maps and the location of errors in these models. *Acta Crystallogr. A* **47**, 110–119.
41. Salemme, F.R., Freer, S.T., Xuong, N.H., Alden, R.A., & Kraut, J. (1973). The structure of oxidized cytochrome c_2 of *Rhodospirillum rubrum*. *J. Biol. Chem.* **248**, 3910–3921.

Received: **29 Mar 1995**; revisions requested: **24 Apr 1995**; revisions received: **10 May 1995**. Accepted: **22 May 1995**.